# The microstructure characteristics of the arc-melted $Gd_5Si_2Ge_2$ alloy

Lei Fang*, Ma Hong

*Communication and Information Engineering Institute, Chongqing University of Posts and Telecommunications, Chongqing, 400065, P. R. China*

Received 27 February 2006, received in revised form 10 May 2006, accepted 10 May 2006

**Abstract**

The $Gd_5(Si_xGe_{1-x})_4$ series alloys are promising candidates for the magnetic refrigeration. The effect of solidification rate on the phase composition and microstructure of the arc-melted $Gd_5Si_2Ge_2$ alloy was investigated in this paper. Three samples with different weight of 10 g, 40 g and 65 g but the same stoichiometric $Gd_5Si_2Ge_2$ composition were prepared by arc-melting using commercial Gd (99.9 wt.%). The X-ray diffraction (XRD) analysis showed that the medium weight sample ($\sim$ 40 g) consists of single $Gd_5Si_2Ge_2$ phase, while the other two samples consist at least of two phases, i.e, $Gd_5Si_4$ and $Gd_5Si_2Ge_2$ phases within our XRD resolution. The cell growth and regular lines within the cell grains are the two main features observed by Scanning-Electron Microscope (SEM) and Optical Microscope (OM) in the as-cast samples. The line features in the medium weight sample were much less developed than those in the other samples. These lines were not confirmed to be the Widmanstätten structure of $Gd_5(Si, Ge)_3$ rods. The melt-spun $Gd_5Si_2Ge_2$ alloy at different wheel speeds confirmed the influence of solidification rates on the phase composition.

PACS: 75.50.Cc; 81.30.Fb

K e y w o r d s: magnetic refrigerating materials, microstructure, $Gd_5Si_2Ge_2$ alloy, magnetic-phase transformation

## 1. Introduction

Magnetic refrigeration is a promising alternative technology for traditional compression refrigeration. Magnetic refrigerating material is one of the most important components in the magnetic refrigeration.

Since some additional lines have been observed in the $Sm_5Ge_3$ X-ray powder diffraction photographs, the 5 : 4 rare earth germanium and silicon compounds were firstly investigated by Smith *et al.* [1] in 1966. They reported the crystallographic data on Nd, Sm, Gd, Tb, Er, and Y 5 : 4 germanides as well as Tb, Er, and Y 5 : 4 silicides using X-ray diffraction (XRD). Their study indicated that all investigated compounds had "the $Sm_5Ge_4$-type structure".

In 1967, Holtzberg *et al.* [2] reported the crystallographic and magnetic data on the heavy rare earth elements Gd, Tb, Dy, Ho, and Er 5: 4 germanides and silicides. The results of XRD analysis of the $Gd_5Si_{4-x}Ge_x$ alloys revealed that: (1) the materials have the $Gd_5Si_4$ structure with some small shift in interplanar spacing $d$ in the composition range from $x = 0$ to 2.0; (2) the $Gd_5Ge_4$ powder pattern was observed from $x =$ 3.0 to 4.0; and (3) new powder pattern not related to either the $Gd_5Si_4$ or $Gd_5Ge_4$ appeared in the range from $x = 2.0$ to 3.0. It was also found that the Curie temperature could be changed from $\sim$ 40 to $\sim$ 300 K by different Si : Ge ratio for the $Gd_5Si_{4-x}Ge_x$ compounds.

The giant magnetic entropy change of the $Gd_5(Si_xGe_{1-x})_4$ alloys was found by Pecharsky *et al.* [3] in 1997. This discovery made the room temperature magnetic refrigeration technology more attractive than ever. The phase relations and the crystallography of the as-cast alloys of a pseudo-binary $Gd_5Si_4$--$Gd_5Ge_4$ system were researched in detail by Pecharsky

*Corresponding author: tel.: 86-23-66231354; fax: 86-23-66231354; e-mail address: leifang06@163.com

in [4]. As a member of the $Gd_5Si_4$-$Gd_5Ge_4$ system, the $Gd_5Si_2Ge_2$ alloy crystallizes in the monoclinic structure (space group $P112_1/a$) and the lattice parameters are $a = 7.5808(5)$, $b = 14.802(1)$, $c = 7.7799(5)$ Å, $\gamma = 93.190(4)^\circ$. The revised magnetic binary diagram based on X-ray powder diffraction, magnetic and thermodynamic measurements of the pseudo-binary $Gd_5Si_4$-$Gd_5Ge_4$ system has been rebuilt by Pecharsky *et al.* [5]. The compounds of the $Gd_5(Si_xGe_{1-x})_4$ system in the region $0.575 \leq x \leq 1$ crystallize in the $Gd_5Si_4$-type structure and they undergo a second order phase transformation with no structural changes. The compounds for $0.4 < x \leq 0.503$ are $Gd_5Si_2Ge_2$--type monoclinic structure and they exhibit a first order phase transformation coupled with the crystallographic phase transformation which has been demonstrated by Morellon *et al.* [6] using X-ray powder diffraction of the $Gd_5Si_{1.8}Ge_{2.2}$ alloy under different temperatures. These compounds exhibit a giant magnetocaloric effect. The third single phase region is $Sm_5Ge_4$-type solid solution when $0 < x \leq 0.3$. The compounds show two phase transitions: the lower temperature magnetic phase transformation coupled with crystallographic phase transition and the higher temperature magnetic phase transformation.

In order to utilize the $Gd_5(Si_xGe_{1-x})_4$ compounds as the work substance in the prototype magnetic refrigerator, establishing the knowledge about the relationships among the process, microstructure, and property is very important. The microstructure of the $Gd_5(Si_xGe_{1-x})_4$ system has also been investigated by some authors. Szade *et al.* [7] first examined the microstructure of $Gd_5Si_4$, $Gd_5Si_2Ge_2$, $Gd_5Ge_4$ single crystals utilizing the scanning electron microscopy (SEM) and the Auger electron microscopy (AES). It was found that the regular parallel line system existed throughout the $Gd_5Si_4$, $Gd_5Si_2Ge_2$ samples. The authors judged that the lines were not grain boundaries or growth steps but formed due to the concentration of impurities taking place along the dislocations. Meyers *et al.* [8] investigated the composition of phases in $Gd_5$ $(Si_{1.95}Ge_{2.05})$ prepared from commercial Gd and found that one of the contaminant phase $Ta_2Si$ and two second phases, $Gd_1(Si, Ge)_1$ and $Gd_5(Si,Ge)_3$ were produced along with the $Gd_5$ $(Si_{1.95}Ge_{2.05})$ matrix. The authors determined by energy dispersive spectroscopy (EDS) that the line features were Widmanstätten structure of $Gd_5(Si, Ge)_3$ rods. However, the sample with the same composition prepared from a high purity Gd had no line feature. Meyers *et al.* [9] also identified the nonmerohedral twinning of $Gd_5Si_2Ge_2$ prepared by 99.8 at.% purity Gd and revealed its twin law based on the transmission electron microscopy (TEM) and selected area diffraction (SAD).

This study aims to determine the phase components and describe the microstructure of the arc-melted $Gd_5Si_2Ge_2$ samples prepared out with different solidification rates. The specific objective is to judge if the line features observed by Meyers *et al.* [8] are Widmanstätten structure of $Gd_5(Si, Ge)_3$ rods.

## 2. Experimental details

Three $Gd_5Si_2Ge_2$ samples, $\sim$ 10 g, $\sim$ 40 g and $\sim$ 65 g, were prepared by arc-melting using commercial 99.9 wt.% pure Gd and $>$ 99.999 wt.% pure Si and Ge in an argon atmosphere. The alloy buttons were re-melted five times to ensure homogeneity. The weight losses of each button during the melting were about 0.5 % and are negligible. Another two samples, each of them $\sim$ 40 g were arc-melted and then rapidly solidified by single-roller melt spinning at wheel speeds of 20 and 50 m/s.

The samples were then analysed by XRD experiments performed on X'Pert Pro MPD X-ray diffractometer (Philips, Netherlands). The voltage and anode current used were 40 kV and 40 mA, respectively. The Cu $K_\alpha = 1.5406$ Å and continuous scanning mode with 0.02 interval and 0.2 second of set time were used to collect the XRD patterns. Qualitative phase analysis was performed with X'Pert HighScore software package (Philips, Netherlands) and PDF2-2003 database (International Center for Diffraction Data, PA, USA). The usage of X'Pert HighScore gives the dynamic match or simulating and obvious marks for matched and unmatched reflections, so that qualitative phase analysis can be easily completed for the multiphase complex mixture with the overlapping reflections. The quantitative phase analysis in X'Pert HighScore works is based on the RIR (Reference Intensity Ratio) values (often called *I/Ic* values). The RIR value is defined as the relative net peak height ratio of the strongest line ($I_{\text{rel}} = 100$ %) of the phase and of the strongest line of corundum, measured with copper $K_\alpha$ radiation in a mixture of equal weight percentages. The set of RIR values is supplied in PDF2 by International Center for Diffraction Data. It determines the mass fractions of the identified phases in a mixture system. This method is known as the normalized RIR method [10–12]. The mass fraction $X\alpha$ of $\alpha$ phase in the mixture is calculated from equation [1]:

$$X\alpha = [I\alpha/RIR\alpha] \times \left[\sum Ii/RIRi\right], \qquad (1)$$

where $RIRi$ is reference intensity ratio of $i^{\text{th}}$ phase of the mixture, and $Ii$ is the intensity of the strongest peak of $i^{\text{th}}$ phase in the analysed mixture. In the X'Pert HighScore, $Ii$ and $RIRi$ are obtained automatically from PDF2 database.

The microstructure was observed by optical microscopy and scanning electron microscopy (SEM)

with energy dispersive spectroscopy (EDS) attached. Samples were examined in the polished and then swiping etched condition for about 10 seconds by the mixture of several kinds of acid, such as lactic acid, phosphorous acid, thick nitric acid, ice acetic acid, oil of vitriol.

The phase transformation temperature near the room temperature was measured by the NETZSCH DSC 204 Differential Scanning Calorimetry (DSC). The samples for the DSC measurements were in the form powders with a weight of 10 mg, which were also used for the XRD experiments.

### 3. Experimental results and discussion

At the bottom of the $Gd_5Si_2Ge_2$ alloy buttons, fine grains were observed distinctly due to the cooling of the water cool copper crucible. From the bottom to the top, the grains gradually grow larger and the belt--like cellular structure can be clearly observed (Fig. 1). Columnar grain boundaries were rich in Si and lean on Gd as demonstrated by our EDS measurements. The cellular solid-liquid interface was clearly observed on the longitudinal sections of samples, as seen in Fig. 2a. The shape of the grains on the transverse section was belt-like (Fig. 2b). So the belt-like cellular grains and the cell wall were defined from the image of the grains. The cells in the ingot were about 50 $\mu$m in width and 200 $\mu$m in length on the longitudinal section. The faster the solidification rate, the narrower and longer the cellular grains are. The parallel line features noted by Szade and Meyers *et al.* [8] were observed within the cells. The lines are about 10–40 $\mu$m in length and 2 $\mu$m in width. It is worth to emphasize that the line system can be easily observed on the longitudinal sections of the button but difficult to be detected on the transverse sections.

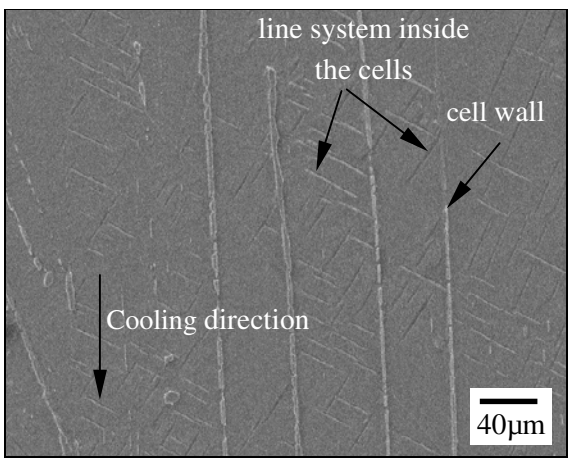


Fig. 1. The typical microstructure of the longitudinal section of the arc-melted $Gd_5Si_2Ge_2$ alloy.

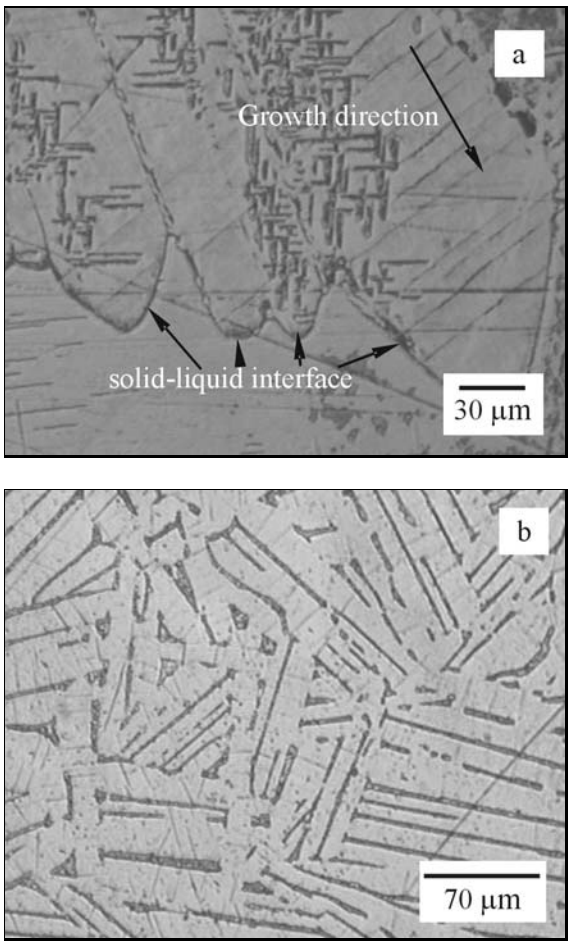


Fig. 2. (a) Solid-liquid interface on the longitudinal section, OM, (b) grain structure on the transverse section, OM.

The X-ray powder patterns of three arc-melted $Gd_5Si_2Ge_2$ alloys in the as-cast condition are shown in Fig. 3. The phase analysis with the help of dynamic match in X'Pert HighScore software shows that the samples with the mass of $\sim$ 10 g and $\sim$ 65 g have orthorhombic $Gd_5Si_4$-type and monoclinic $Gd_5Si_2Ge_2$--type double phases and the sample with the weight of $\sim$ 40 g has monophasic monoclinic $Gd_5Si_2Ge_2$--type phase. Table 1 shows the quantitative analysis of $Gd_5Si_2Ge_2$ samples with different weight. The RIR values of $Gd_5Si_2Ge_2$ and $Gd_5Si_4$ are from PDF2--2003 database. Theoretically RIR quantitative analysis method should give the exact results of quantitative analysis. Practically speaking, several sources of errors may lead to inaccurate results. The main errors are believed to be: (i) the RIR values from the reference database and (ii) overlapping of the strongest reflection that will result in the wrong intensity for each phase. In order to obtain the intensity of $Gd_5Si_2Ge_2$ and $Gd_5Si_4$ phases, the deconvolution of overlapping

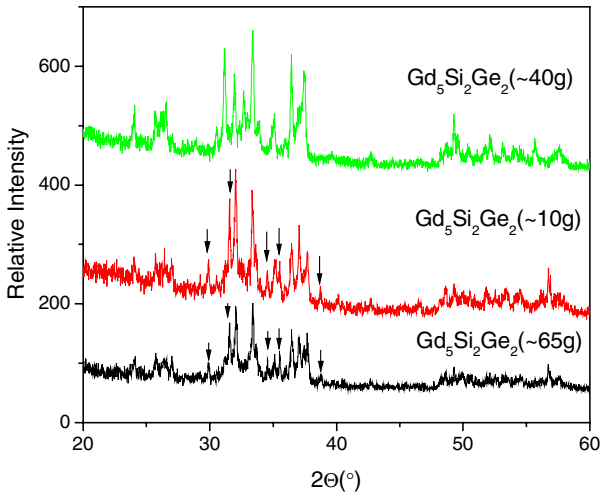


Fig. 3. XRD patterns of the arc-melted $Gd_5Si_2Ge_2$ alloys with different weight. The sample with ∼ 40 g weight has the single monoclinic $Gd_5Si_2Ge_2$-single phase. The other two samples have double-phase structure including the orthorhombic $Gd_5Si_4$-type phase (indicated by down arrows) and the monoclinic $Gd_5Si_2Ge_2$-type phase.

diffraction lines was processed with profile-fit based Voigt function constructed in the X'Pert HighScore.

In order to verify the correction of the qualitative phase analysis, two samples of ∼ 65 g and ∼ 40 g $Gd_5Si_2Ge_2$ were selected for the phase transformation temperature measurements in temperature range from −40 ℃ to 50 ℃ by Differential Scanning Calorimetry (DSC). It can be seen in Fig. 4 that the DSC curve of the 65 g $Gd_5Si_2Ge_2$ sample shows three peaks. The two lower temperature nearly overlapped peaks correspond to the monoclinic $Gd_5Si_2Ge_2$-type phases at room temperature, which have different but close Si : Ge ratio. So the ∼ 65 g sample undergoes three phase transitions on heating, two continuous first order ferromagnetic to paramagnetic phase transformation coupled with the $Gd_5Si_4$-type to $Gd_5Si_2Ge_2$-type crystallographic phase change near −1.8 ℃ (271.2 K) and the higher temperature second order ferromagnetic to paramagnetic phase transformation near 23.6 ℃ (296.6 K). The ∼ 40 g $Gd_5Si_2Ge_2$ sample exhibits only one sharp peak which corresponds to the first order transformation as that of the ∼ 65 g $Gd_5Si_2Ge_2$ sample near 3.1 ℃ (276.1 K). It is clearly indicated that the ∼ 65 g $Gd_5Si_2Ge_2$ sample contained $Gd_5Si_2Ge_2$-type and $Gd_5Si_4$-type phases, while the ∼ 40 g $Gd_5Si_2Ge_2$ contained monophasic $Gd_5Si_2Ge_2$--type phase at room temperature and that was in accordance with the XRD analysis.

Table 1. Weight fractions of arc-melted $Gd_5Si_2Ge_2$ alloys with different weight calculated with RIR method

| Weight fraction | $Gd_5Si_2Ge_2$ (∼ 10 g) | $Gd_5Si_2Ge_2$ (∼ 40 g) | $Gd_5Si_2Ge_2$ (∼ 65 g) |
|---|---|---|---|
| $Gd_5Si_4$-type phase (%) | 24 | 0 | 22 |
| $Gd_5Si_2Ge_2$-type phase (%) | 76 | 100 | 78 |

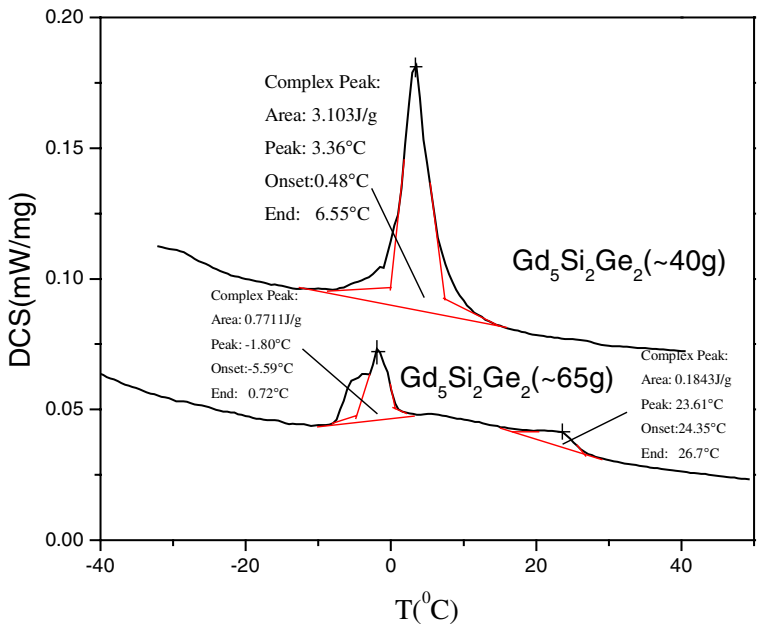


Fig. 4. Phase transformation temperature measured by the DSC. $Gd_5Si_2Ge_2$ sample with ∼ 40 g weight has one first order phase transformation, the other sample with ∼ 65 g weight has two first order phase transformations and one second order phase transformation.

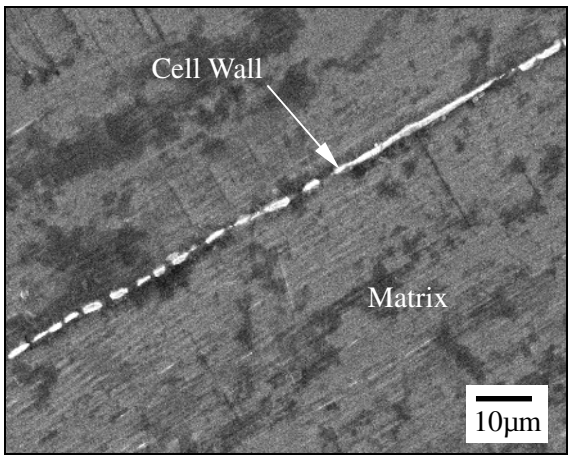


Fig. 5. Microstructure of the sample with ∼ 40 g weight. Nearly no "line features" can be seen from the image.

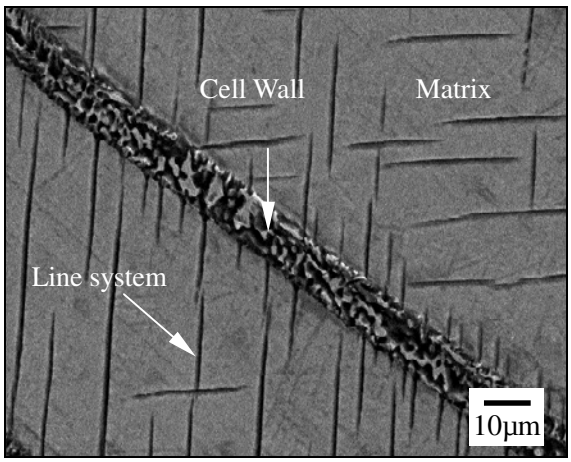


Fig. 6. Microstructure of the sample with ∼ 10 g weight. Large amounts of line features and broader cellular walls can be seen.

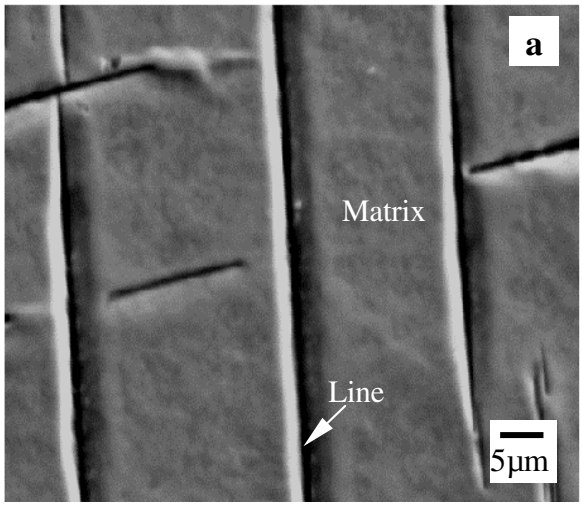


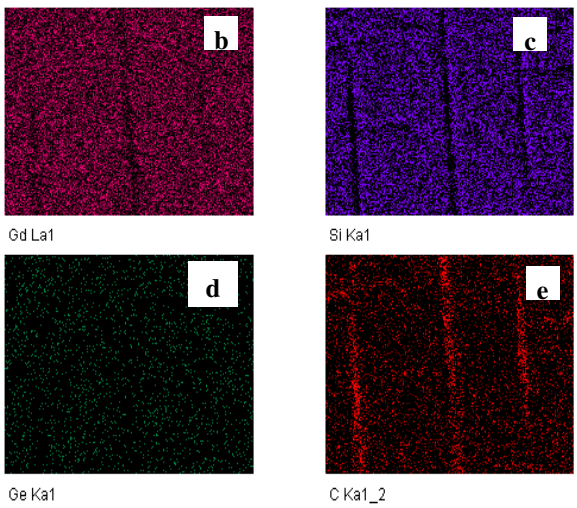


Fig. 7. (a) SEM image of the lines within the cellular grain of the sample with ∼ 65 g weight, (b–e) corresponding EDS mapscans.

The microstructure images of the three ∼ 40 g, ∼ 10 g, and ∼ 65 g $Gd_5Si_2Ge_2$ samples are shown in Figs. 5–7, respectively. It can be seen in these images that the ∼ 40 g $Gd_5Si_2Ge_2$ nearly has no line features. It resembles to that of the $Gd_5Si_2Ge_2$ using high purity 99.9 at.% Gd in [8]. The cell walls in Fig. 5 are narrower than that in the ∼ 65 g. The ∼ 65 g and ∼ 10 g $Gd_5Si_2Ge_2$ have large amounts of lines inside the cells (Figs. 6 and 7a). Especially for the ∼ 10 g $Gd_5Si_2Ge_2$ sample, the cell walls were broader than those of the other two samples. The EDS linescans were performed along the directions perpendicular to the walls (Fig. 8). A drop in Gd and a corresponding increase in Si, C, O can be seen in the walls, while no visible change was detected in Ge.

To make clear the nature of the line system in $Gd_5Si_2Ge_2$, mapscans were performed in the field of view (Figs. 7b–e). It is worth noting that measuring

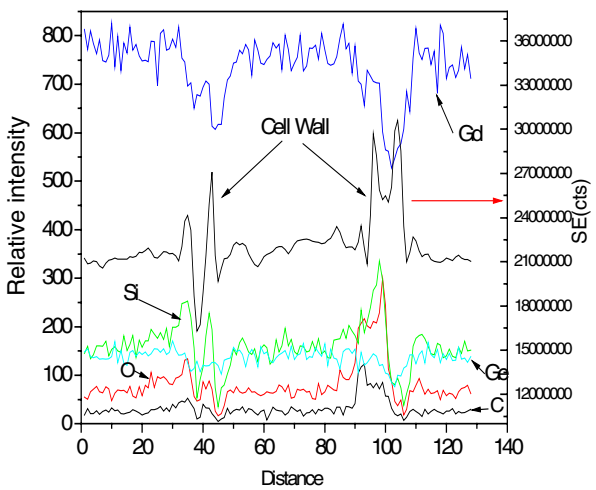


Fig. 8. EDS linescans perpendicular to the cellular walls.

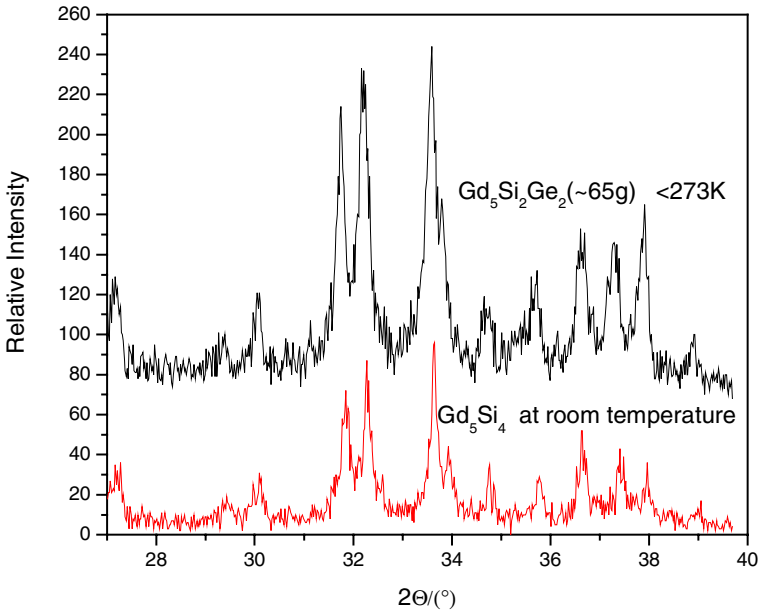


Fig. 9. Low temperature XRD pattern of the $Gd_5Si_2Ge_2$ sample with ~ 65 g weight and the pattern of the room temperature $Gd_5Si_4$ alloy. Only orthorhombic $Gd_5Si_4$-type phase exists at low temperature for the measured $Gd_5Si_2Ge_2$ sample.

the point composition by EDS on the lines (channels) is not appropriate because they are too narrow. The distributions of Gd, Si, Ge and impurity C are shown in Figs. 7b–e. The other detected impurities O and Ca, P, Cl had the same distribution characteristics as C and were not listed. The impurities of P, Cl were from the etching acid. Elements such as Ca were from the raw materials and C, O were from the raw materials, the contamination during the melting, and surface absorption. It can be seen from the mapscans that there is a drop (the colour is darker in the channels than that in the matrix) in Gd and Si in the channels and a corresponding increase (the colour is brighter in the channels than that in the matrix) in the impurities C, O, Ca, P, Cl. No particular fluctuation in Ge was observed. The result of the dropping of Gd in the channels is different from that of Meyer's [8] which indicates that the line features do not correspond to the $Gd_5(Si, Ge)_3$-type phase whose content of Gd is by 7 at.% higher than that of the $Gd_5Si_2Ge_2$ matrix. Moreover, in order to demonstrate the lack of $Gd_5(Si, Ge)_3$-type phase, the low temperature ($< 273$ K) XRD was performed (Fig. 9). The XRD pattern shows also evidence of monophasic $Gd_5Si_4$ phase. The room temperature $Gd_5Si_2Ge_2$-type phase transforms to $Gd_5Si_4$--type on cooling but there is no transition for the $Gd_5(Si, Ge)_3$ phase due to its very low $T_N$ [13]. If there is some $Gd_5(Si, Ge)_3$ phase in the alloy, the patterns of $Gd_5(Si, Ge)_3$-type phase should be retained at low temperature during cooling. The $Gd_5(Si, Ge)_3$-type phase can be easily detected even if its content is low in the alloy because the relative intensity of its XRD pattern is ten times higher than that of $Gd_5Si_2Ge_2$-type or $Gd_5Si_4$-type phases under the same scanning condition. From Fig. 9, monophasic $Gd_5Si_4$-type phase was detected at temperature under 273 K. This illustrates the absence of $Gd_5(Si, Ge)_3$ phase in room temperature. This method eliminates the overlapping of the characteristic peak of $Gd_5(Si, Ge)_3$ phase with that of the $Gd_5Si_2Ge_2$-type phase at $2\theta = \sim 35°$. Since the line system was not identified to be Widmanstätten $Gd_5(Si, Ge)_3$ phase, further analysis was performed. Assuming that the $Gd_5Si_2Ge_2$ with monophasic structure had no line features but the diphase $Gd_5Si_2Ge_2$ alloys had many, the lines in the microstructure may be the $Gd_5Si_4$-type phase. However accurate definition needs electron diffraction of TEM. The difficulty of this work lies in the sample preparation because of the friability of the $Gd_5(Si_xGe_{1-x})_4$ compounds.

Pecharsky *et al.* [5] emphasized that in order to ensure the homogeneity of the arc-melted buttons and avoid the formation of neighbouring phases of $Gd_5(Si, Ge)_4$, the weight of alloys should not exceed 25 g. According to our experiments, we found that the button weight had effect on the coexistence of the monoclinic $Gd_5Si_2Ge_2$-type phase with the orthorhombic $Gd_5Si_4$--type phase. Considering the difference of the solidification rates of the arc-melting furnace and the purity of the raw materials, we determined that the phase selection during the solidification was controlled at least by both solidification rates and the impurities. In order to further survey the effect of solidification rates on the phase selection of $Gd_5Si_2Ge_2$, single-roller melt spinning processes were employed. This process can ensure the homogeneity of the alloys and give the results of the effect of solidification rates on the phase composition. Figure 10 showed the XRD pattern of melt--spun $Gd_5Si_2Ge_2$ under different wheel speeds. The

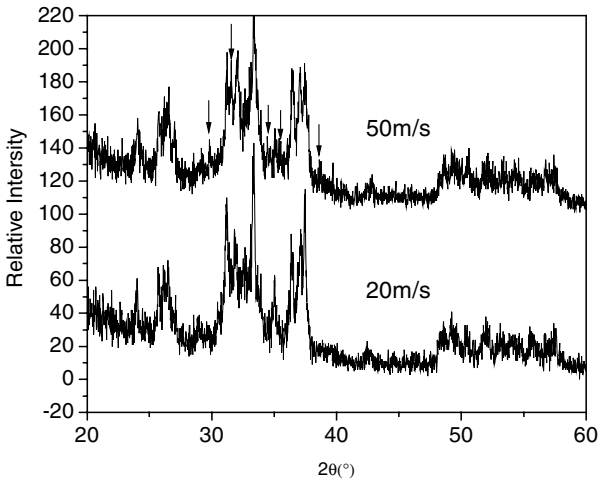


Fig. 10. The XRD patterns of the melt-spun $Gd_5Si_2Ge_2$ alloys at different wheel speeds. The sample prepared at 50 m/s has the orthorhombic $Gd_5Si_4$-type (indicated by down arrows) and monoclinic $Gd_5Si_2Ge_2$ phases, while the sample prepared at 20 m/s has the monoclinic $Gd_5Si_2Ge_2$ phase.

$Gd_5Si_2Ge_2$ prepared at speed of 50 m/s had the orthorhombic $Gd_5Si_4$-type and monoclinic $Gd_5Si_2Ge_2$--type phases, while the $Gd_5Si_2Ge_2$ prepared at 20 m/s had the monoclinic $Gd_5Si_2Ge_2$-type structure. This demonstrates the effect of solidification rates on the phase selection of stoichiometric $Gd_5Si_2Ge_2$ alloy.

## 4. Conclusions

The present study confirmed that the cellular growth and regular lines within the grains are the two main characteristics in the arc-melted $Gd_5Si_2Ge_2$. Solidification rates had important impact on the final phase composition and microstructure of the arc--melted $Gd_5Si_2Ge_2$ alloy. Multi-phases including orthorhombic $Gd_5Si_4$-type and monoclinic $Gd_5Si_2Ge_2$--type phases can be obtained at the fastest or slowest cooling rates by arc melting. The regular lines were not confirmed to be Widmanstätten structure of $Gd_5(Si, Ge)_3$ rods.

## References

[1] GORDON, S.—SMITH, A.—THARP, G.—JOHSON, Q.: Nature, *21*, 1966, p. 1148.
[2] HOLTZBERG, F.—GAMBINO, R. J.—McGUIRE, T. R.: J. Phys. Chem. Solids, *28*, 1967, p. 2283.
[3] PECHARSKY, V. K.—GSCHNEIDNER, K. A., Jr.: Physical Review Letters, *78*, 1997, p. 4494.
[4] PECHARSKY, V. K.—GSCHNEIDNER, K. A., Jr.: J. alloys and compounds, *260*, 1997, p. 98.
[5] PECHARSKY, A. O.—PECHARSKY, V. K.—GSCHNEIDNER, K. A., Jr.: J. alloys and compounds, *338*, 2002, p. 126.
[6] MORELLON, L.—ALGARABEL, P. A.—IBARRA, M. R. et al.: Phys Rev B, *58*, 1998, R14721.
?[7]? GSCHNEIDNER, K. A., JR.—PECHARSKY, A. O.—PECHARSKY, V. K.—LOGRASSO, T. A.—SCHLAGEL, D. L.: In: Rare Earth and Actinides: Science, Technology and Applications IV. Eds.: Bautista, R. G., Mishra B. Warrendale, PA, TMS 2000, p. 63.
?[7]? SZADE, J.—SKOREK, G.—WINIARSKI, A.: J. Cryst. Growth, *205*, 1999, p. 289.
[8] MEYERS, J. S.—CHUMBLEY, J. S.—LAABS, F.—PECHARSKY, A. O.: Scripta Materialia, *47*, 2002, p. 509.
[9] MEYERS, J.—CHUMBLEY, S.—CHOE, W.—MILLER, G. J.: Phys Rev B, *66*, 2002, p. 012106-1.
[10] CHUNG, F. H.: J. Appl. Cryst., *7*, 1974a, p. 513.
[11] CHUNG, F. H.: J. Appl. Cryst., *7*, 1974b, p. 526.
[12] CHUNG, F. H.: J. Appl. Cryst., *8*, 1975, p. 17.
[13] CANEPA, F.—CIRAFICI, S.—NAPOLETANO, M.: Journal of alloys and compounds, *335*, 2002, p. L1.